Chapter 4

Results and Discussions

4.1 Powder Characterization

PZT powder prepared by mixed oxide route and 40/30 commercial PZT powder were calcined at several temperatures and analysed by x-ray diffractometry to identify the phase change of the samples. The particle sizes of the powder were determined by the methods, the details of which and their results were shown in next sections. These properties of PZT powder are of importance for use as filler phase in 0-3 piezoceramic polymer composite.

4.1.1 X-ray Diffraction Results

The PZT powder calcined at the temperatures of 400 °C, 500 °C, 600 °C, 700 °C, 800 °C, 900 °C, 1000 °C, 1100 °C, 1200 °C and 1300 °C was scanned using a Jeol Diffractometer with Ni filtered CuK_α radiation, covering the 2θ ranges of

15°-60° , stepping scan of 0.5° and 1 sec counting time per step was employed. The corresponding diffractograms were compared with JCPDS powder diffraction file of PZT powder[1] as shown in Table 4.1. Every crystalline substance has a unique x-ray powder pattern because the line position depends on the unit cell size while line intensity depends on the type of atom present on the diffraction planes and their arrangement in the crystal. Therefore an unknown solid powder can be identified from its unique powder pattern[2]. Figure 4.1 shows the x-ray diffraction pattern of mixed oxide PZT powder calcined at various temperatures. The X-ray diffractograms indicated that all the samples correspond to PZT[1]. No impurity was found by this method. However a little unknown peak (d = 3.195 Å) was present. This is probably due to the diffraction caused by the remaining of the CuK_β after Ni filtering. The line splitting (100) into (100) and (001) peaks showed that the tetragonal phase appeared between 1100-1200 °C, whereas the cubic phase existed at the lower temperatures. Therefore, annealing at 1100, 1125, 1150, 1175 and 1200 °C was carried out again and the samples

Table 4.1 JCPDS Powder Diffraction File[1] of PZT powder.

d(Å)	I/I_1	hkl
4.146	9	001
4.036	12	100
2.890	100	101
2.850		110
2.351	15	111
2.073	9	002
2.018	16	200
1.844	5	102
1.810	6	201, 210
1.677	12	112
1.655	25	211
1.446	9	022
1.427	5	220
1.382	2	003
1.361	6	212
1.350		221
1.038	6	103
1.244	2	113
1.220	2	311

were re-examined in details with 2θ ranges of 20.75°-23.00° at (100) and (001) peaks, 0.01° of scanning step and 2 sec counting time was employed. Figure 4.2 shows the X-Ray profiles of the peaks (100) and (001) of the samples at the annealing temperatures of 1000 to 1200 °C. It can be concluded that transformation of the cubic to the tetragonal phase starts at 1125 °C, and was most pronounced at 1200 °C. Tetragonallity (c/a) was also calculated using Cohen's method[3], those being 1.009, 1.012, 1.014 and 1.016 for annealing temperatures of 1125, 1150, 1175 and 1200 °C, respectively.

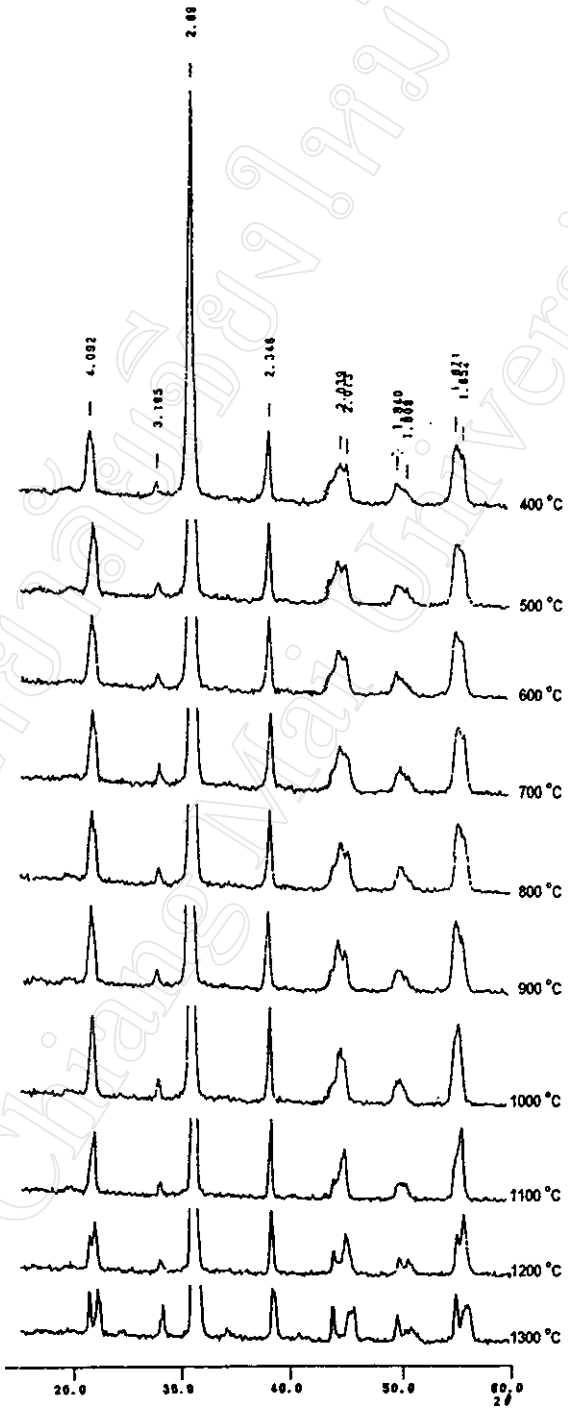

Figure 4.1 XRD of PZT powder annealed at several temperatures.

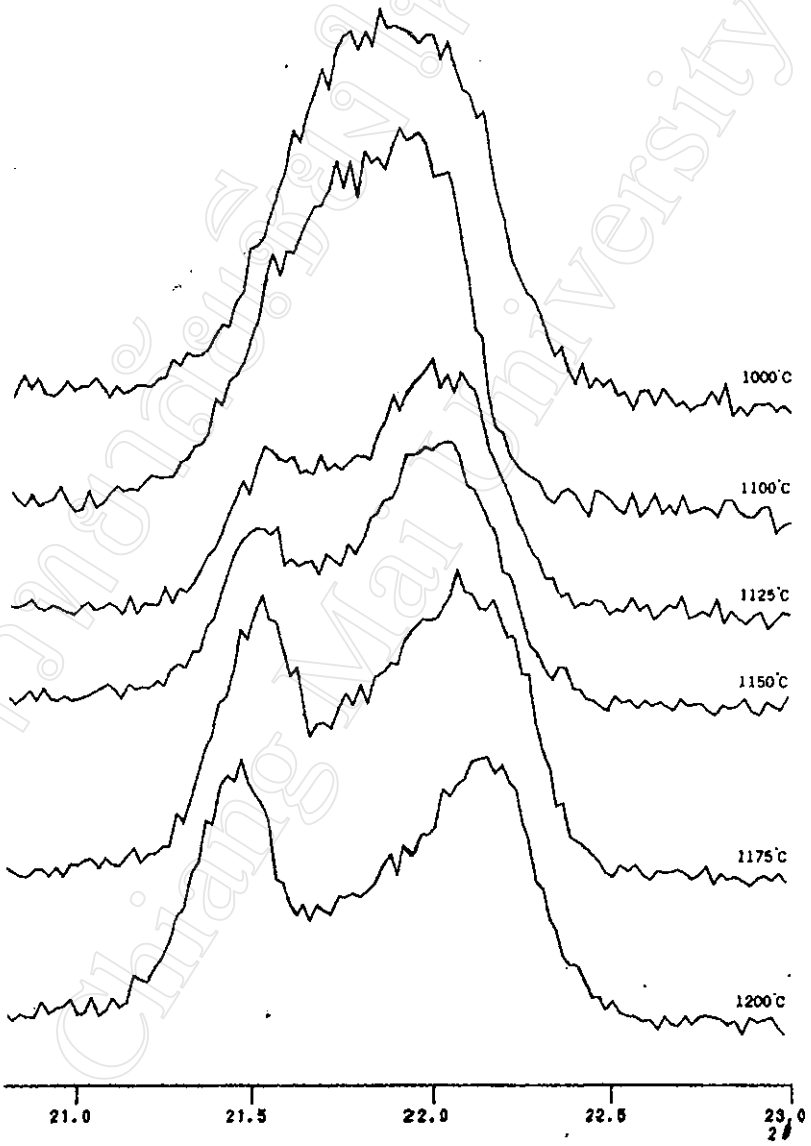

Figure 4.2 XRD pattern of the (100) and (001) peaks of PZT powder annealed at the temperatures of 1000, 1100, 1125, 1150, 1175 and 1200 °C.

4.1.2 Determination of the Particle Size

4.1.2.1 Measuring by a Sedimentograph

Both PZT powders which were prepared by the solid state reaction and commercial 40/30 powder were annealed at the temperature of 1200 °C, sieved through mesh number 100 and 300, and scanned using a Shimazu sedimentograph. Figures 4.3 -4.4 show distribution curves of the particle size of PZT powders. The arithmatic mean of the particle size were 150 μm, 62 μm, 159 μm and 55 μm for

a) The mixed oxide PZT powder sieved through mesh number 100,

b) The mixed oxide PZT sieved through mesh number 300,

c) The 40/30 PZT powder sieved through mesh number 100, and

d) The 40/30 PZT powder sieved through mesh number 300.

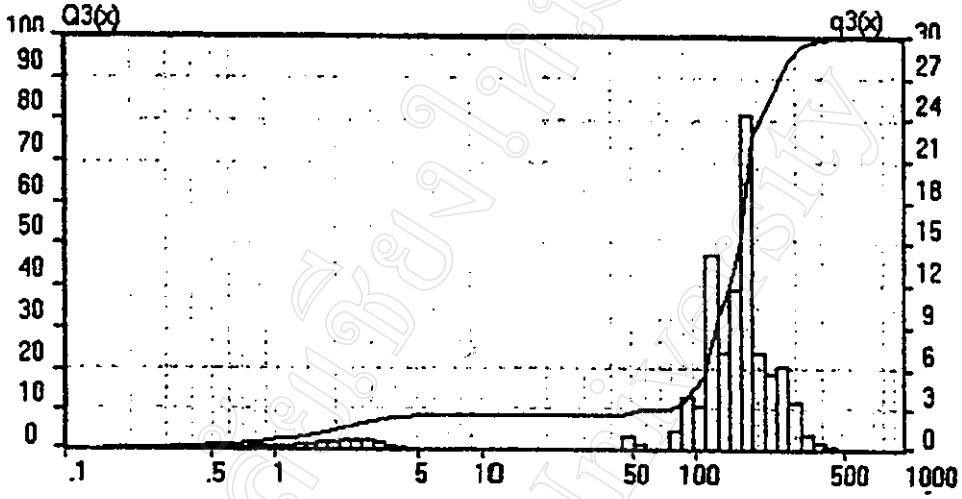

(a)

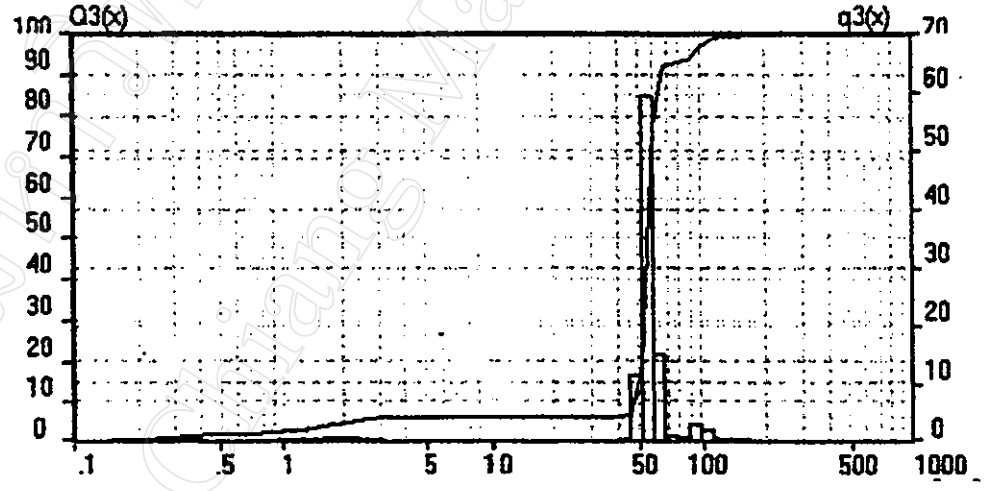

(b)

Figure 4.3 Particle size distribution curve of 40/30 PZT powder: (a) sieved through mesh number 100 and (b) sieved through mesh number 300.

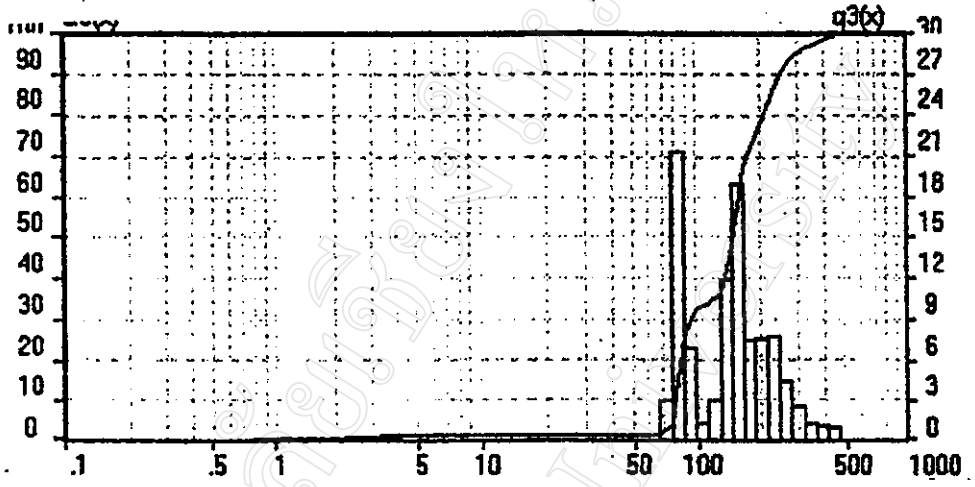

(a)

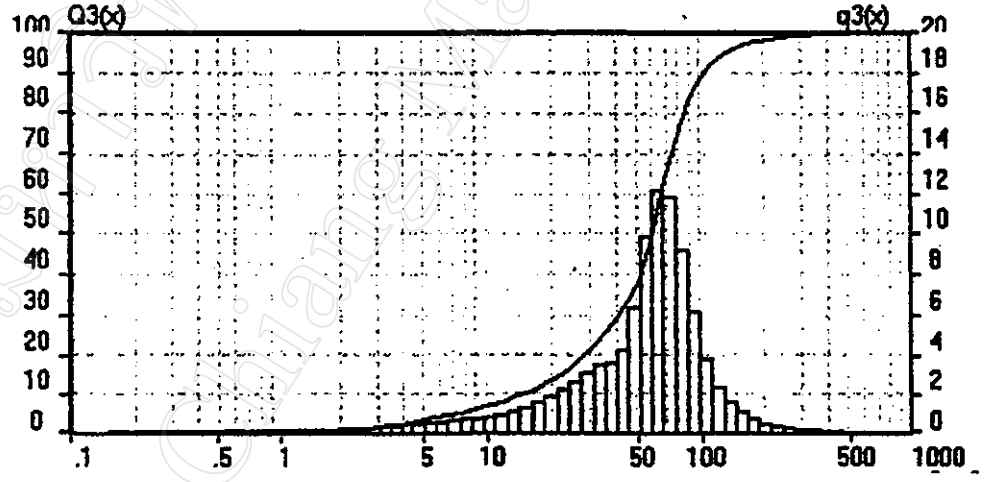

(b)

Fugure 4.4 Particle size distribution curve of mixed oxide PZT powder: (a) sieved through mesh number 100 and (b) sieved through mesh number 300.

4.1.2.2 Determination of the X-Ray Line Profile Using the Fourier Method

The X-ray line profile of the peak (111) of PZT powder calcined at temperatures of 400 °C - 1300 °C was scanned slowly inorder to study the line broadening as shown in Figure 4.5. The data of line profiles (2θ versus intensity) were computed using a computer program to estimate the particle size and microstrain of the samples. The program was written in basic programing language (Appendix A) following the method in Section 3.3.1.3. Figure 4.6 and 4.7 show the variation of the Fourier coefficient ($I_{re}(t)$) of the samples as a function of the harmonic number n, where n is the particular Fourier series under consideration. The value of n is related to the length L normal to the reflecting plane of the interplanar spacing d_{hkl} by $L = nd_{hkl}$. The particle sizes and microstrains were calculated for each annealing step and plotted in Figure 4.8. The microstrain decreased slowly with the temperature up to about 900 °C with the little increase in particle size. At annealing temperatures above 900 °C, the microstrain showed rapid decrease while the

particle size increased by a factor of four. Beyond an annealing temperature of 1100 °C, the change of both microstrain and particle size were almost constant.

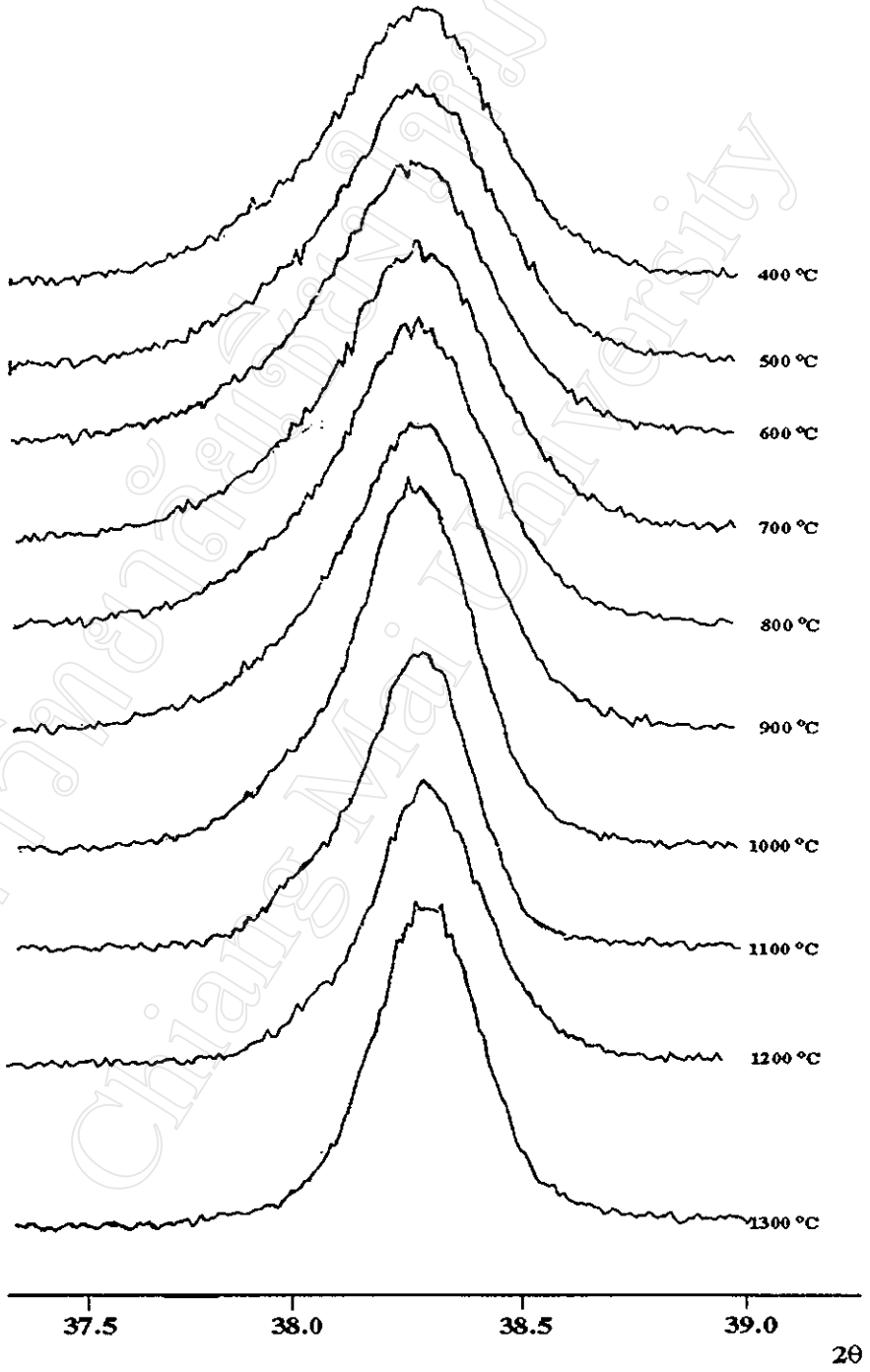

Figure 4.5 X-ray diffraction pattern of the peak (111) of PZT powder annealed at different temperatures.

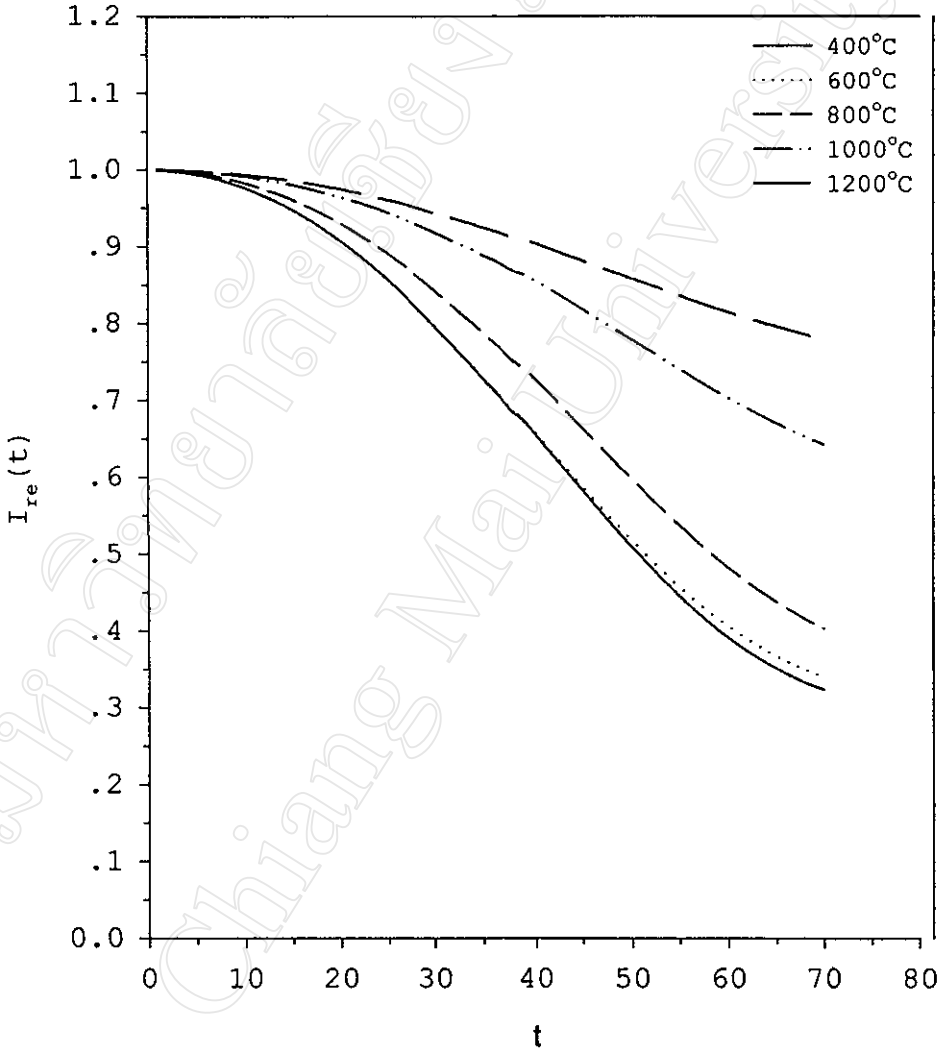

Figure 4.6 Variation of the Fourier coefficient $I_{re}(t)$ with t of PZT powder annealed at temperatures of 400, 600, 800, 1000 and 1200 °C.

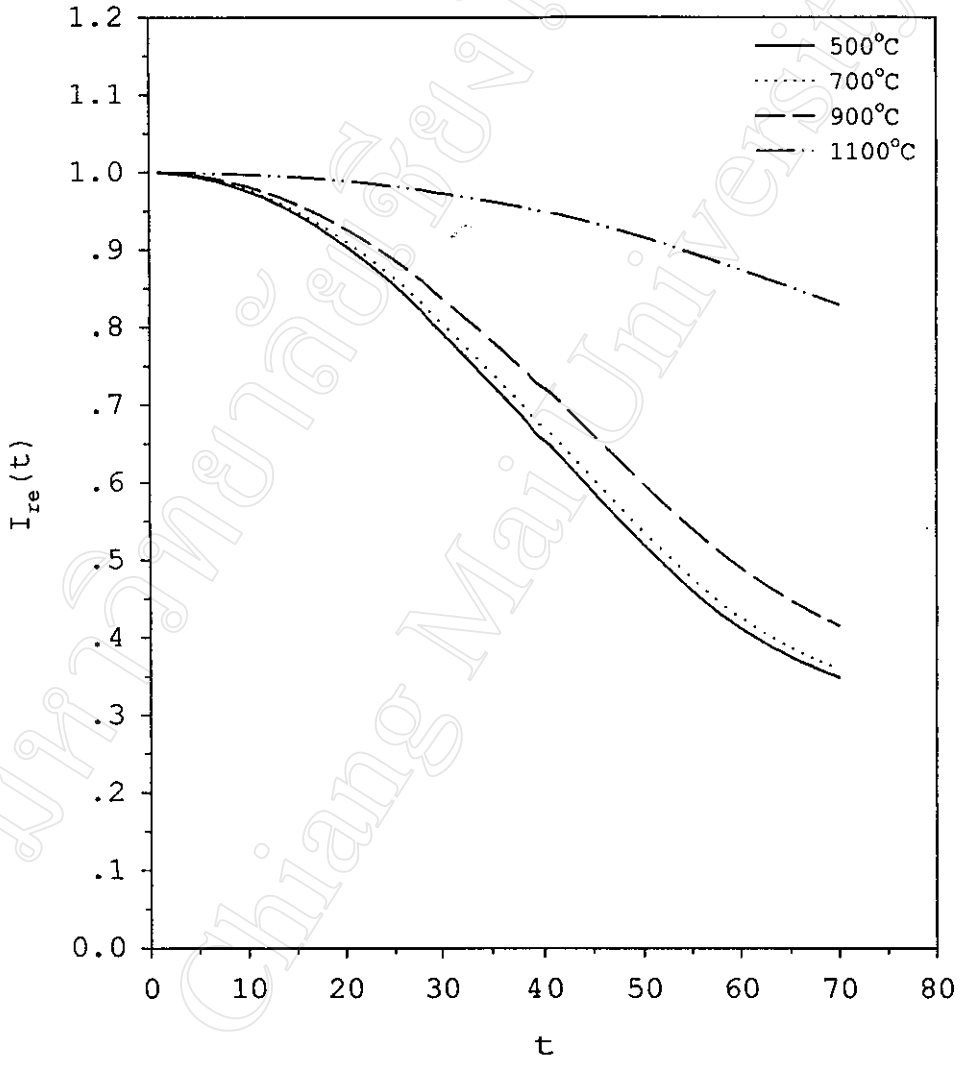

Figure 4.7 Variation of the fourier coefficients $I_{re}(t)$ with t of PZT powder annealed at temperatures of 500, 700, 900, and 1100 °C.

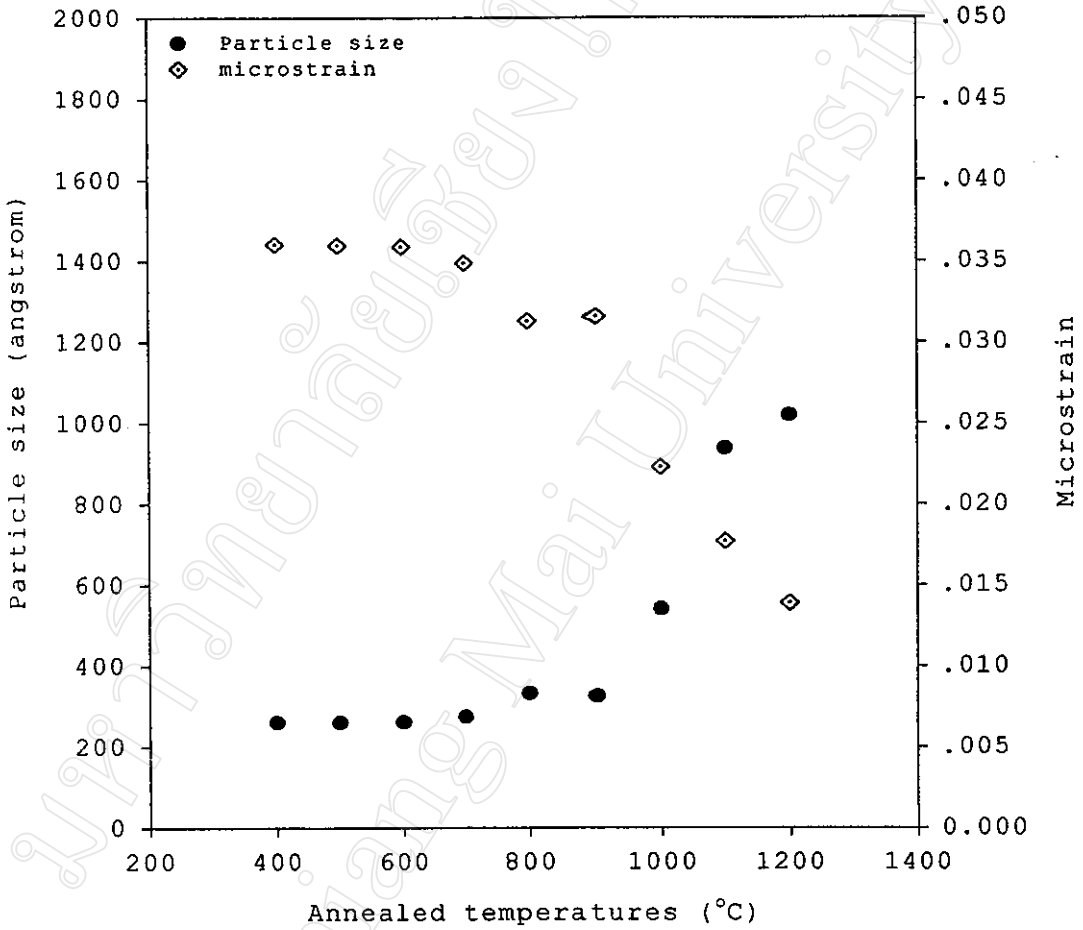

Figure 4.8 Particle size and microstrin of PZT powder as a function of the annealing temperatures.

4.1.2.3 Measuring by Scanning Electron Microscopy

The scanning electron micrographs of PZT powder calcined at different temperatures were shown in Figures 4.9-4.18.

Figure 4.9 Scanning electron micrograph of PZT powder calcined at 400 °C.

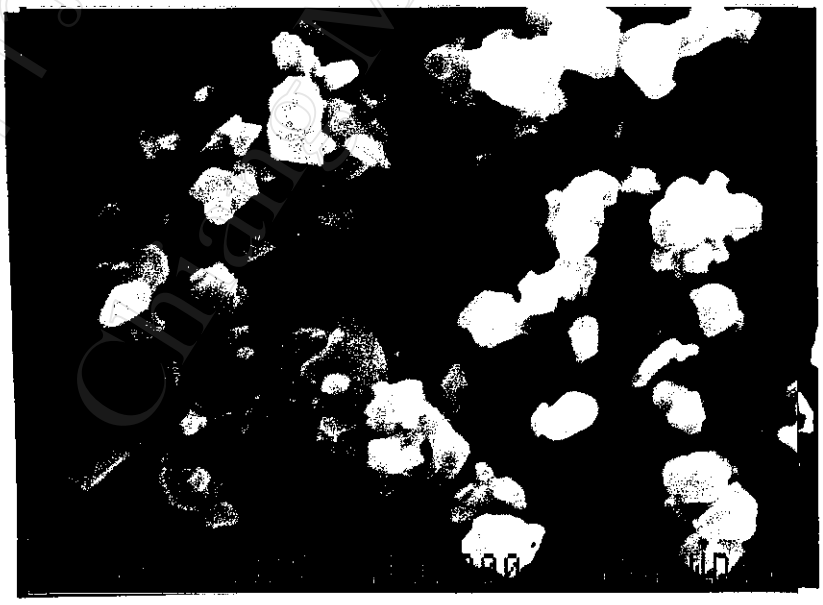

Figure 4.10 Scanning electron micrograph of PZT powder calcined at 500 °C.

Figure 4.11 Scanning electron micrograph of PZT powder calcined at 600 °C.

Figure 4.12 Scanning electron micrograph of PZT powder calcined at 700 °C.

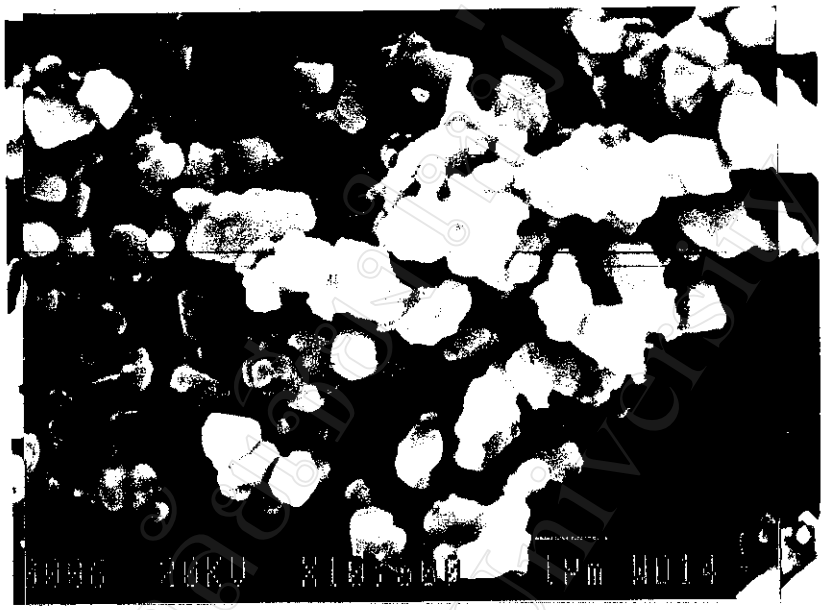

Figure 4.13 Scanning electron micrograph of PZT powder calcined at 800 °C.

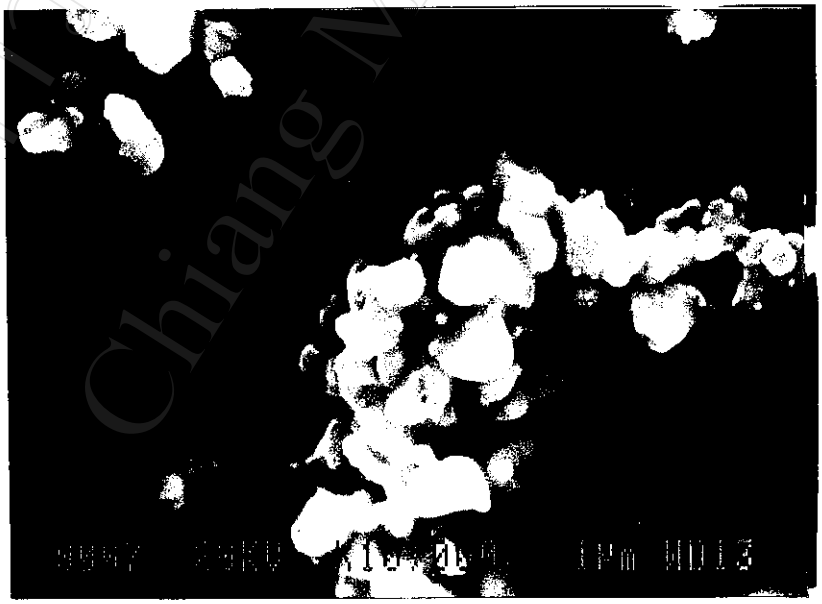

Figure 4.14 Scanning electron micrograph of PZT powder calcined at 900 °C.

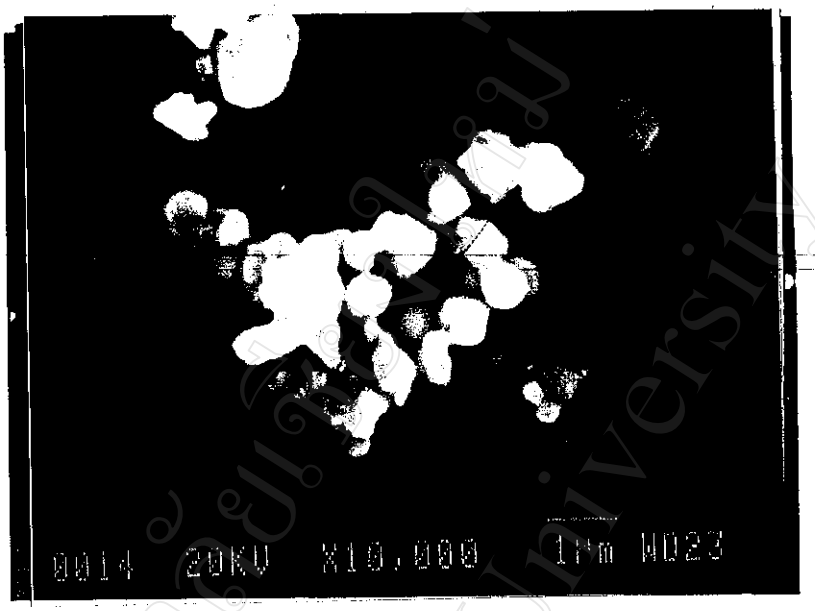

Figure 4.15 Scanning electron micrograph of PZT powder calcined at 1000 °C.

Figure 4.16 Scanning electron micrograph of PZT powder calcined at 1100 °C.

Figure 4.17 Scanning electron micrograph of PZT powder calcined at 1200 °C.

Figure 4.18 Scanning electron micrograph of PZT powder calcined at 1300 °C.

Figures 4.9-4.18 indicate that the morphology of particles of PZT powder which are not spherical. This may be due to the powder were ball-milled before calcine. The sizes of PZT particles of the calcined samples are measured at each temperature. The average particle sizes of the powder are shown in Table 4.2. It was found that the size of particle slowly increases with increasing of the calcine temperature

Table 4.2 The average particle sizes of PZT powder measured from SEM.

Calcine temperature (°C)	Average particle size (μm)
400	0.67
500	0.78
600	0.81
700	0.78
800	0.94
900	1.00
1000	1.05
1100	1.33
1200	1.61
1300	1.55

4.2 Properties of 0-3 Piezoceramic-Polymer Composites

4.2.1 Density

The density of all composite samples were measured using Archimedes principle and tabulated in the Table 4.3. The volumetric fraction of PZT particles in composites were measured using Equation (3.20). The variation of density against volumetric fraction was plotted in Figures 4.19-4.21. It was found that the density linearly increases with the increasing of volumetric fraction. This result correspond to Equation (3.20). In the same volumetric fraction, the density of the composites prepared from the centrifuge method using 40/30 and mixed oxide PZT close together while the density of composites prepared from conventional is lower than that prepared in a centrifuge. This is probably due to the difference of the polymer matrix density, that is, the density of PE (0.92 g/cm^3) is lower than that of polyester resin (1.17 g/cm^3). The measured volumetric fractions of the composites are little different from the expected volumetric fractions. The error of volumetric fraction in conventional composites appears to be lower than that obtained from the centrifuging composites. This may be due to relatively

more precisely control the ratios of ceramic to polymer in conventional method(Appendix C).

Table 4.3 Density of the 0-3 composites.

Samples	Vol%	Density (g/cm^3)	Measured Vol%	Error of Vol%
Conventional	10	1.1620	10.17	1.70
40/30 PZT+PE	20	2.324	20.40	2.00
	30	3.044	30.87	2.90
	40	3.670	39.97	0.08
	50	4.516	52.26	4.52
	60	5.026	59.68	0.53
Centrifuge	40	3.612	39.19	2.03
PZT(obtain from	50	4.290	50.01	0.02
mixed oxide	60	4.850	59.01	1.57
route)+resin	65	5.210	64.52	0.74
Centrifuge	40	3.690	39.19	2.03
40/30 PZT+resin	50	4.361	49.62	0.76
	60	5.045	60.26	0.43
	65	5.290	64.07	1.43

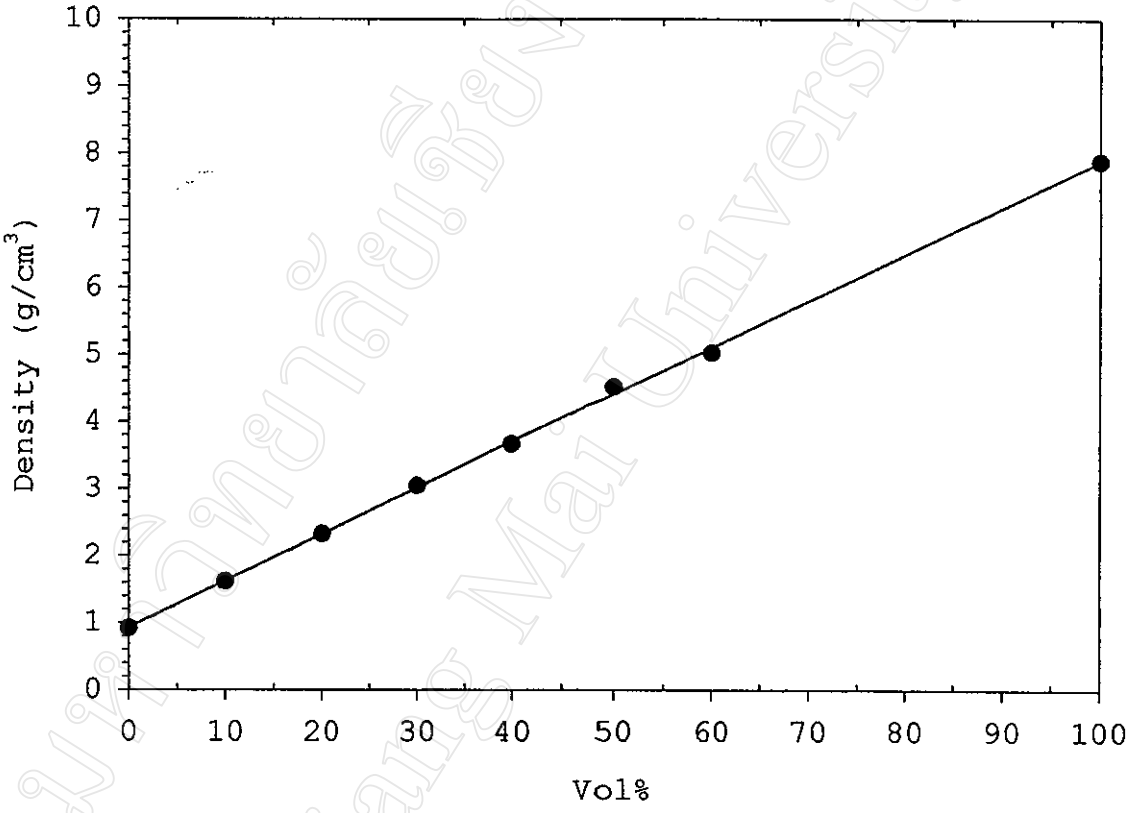

Figure 4.19 The density of conventional PE and 40/30 PZT composites as a function of ceramic volume percentage.

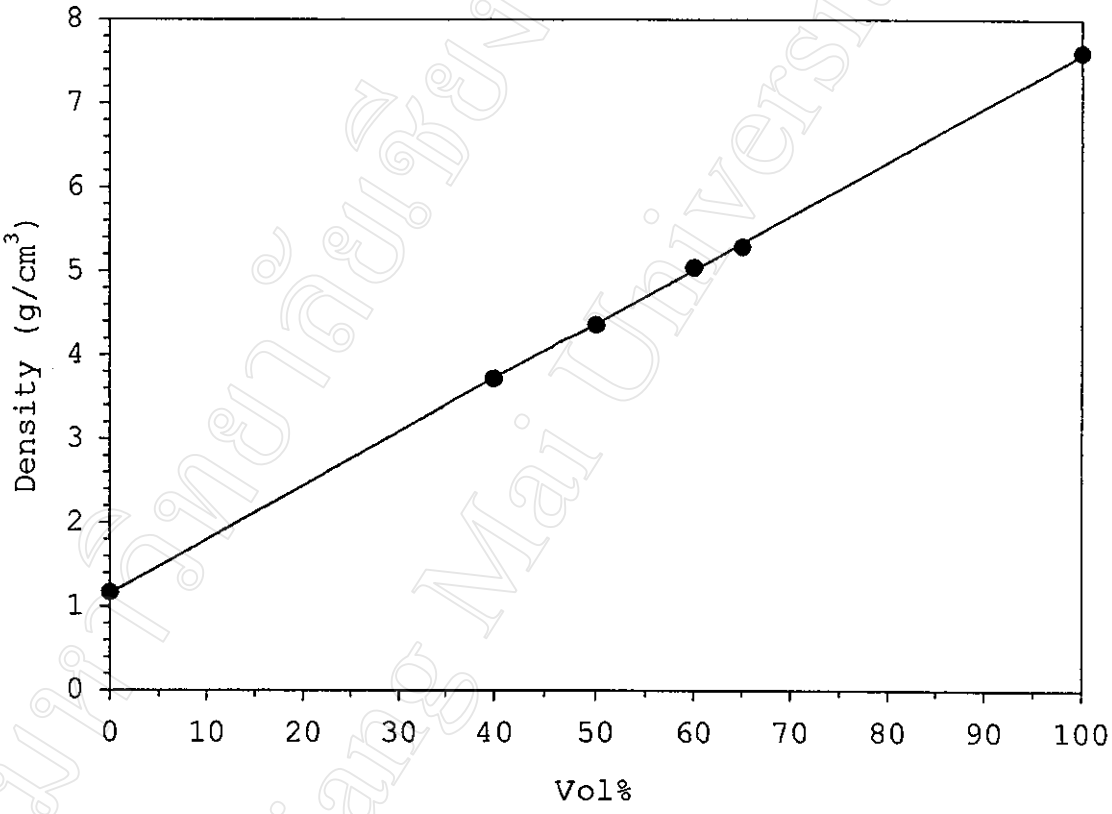

Figure 4.20 The density of centrifuging resin and 40/30 PZT composites as a function of ceramic volume percentage.

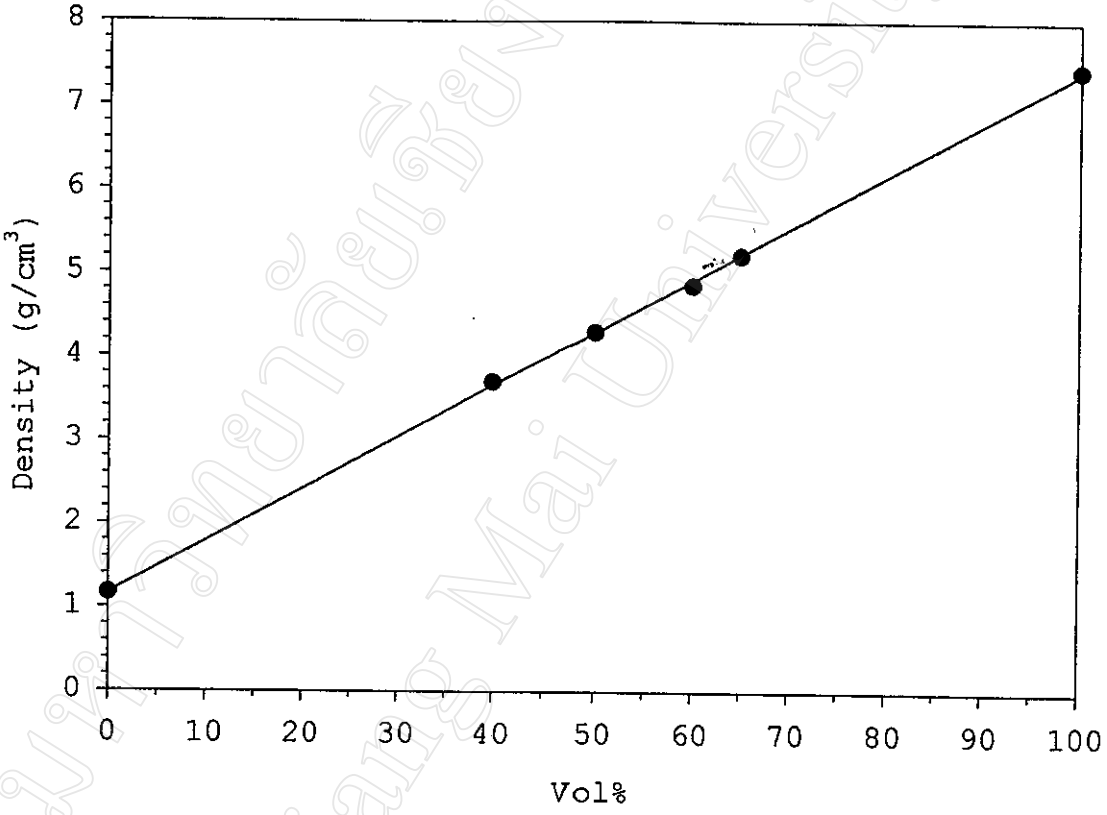

Figure 4.21 The density of centrifuging resin and mixed oxides PZT powder composites as a function of ceramic volume percentage.

4.2.2 Scanning Electron Micrographs of Composites

Figures 4.22-4.25 show scanning electron micrographs of the distribution of PZT powder in the composite. The fabrication by the centrifuging method shows a considerably good distribution of the ceramic particles in the polymer phase. The PZT powder at the higher volume fraction samples seem to pack closer and denser than that in the lower volume fraction samples. It is difficult to see the distribution of ceramic powder at the surface of the conventional mixing samples because of the interference of fiber hair in PE after polishing.

4.2.3 Dielectric Properties

The dielectric constant (ε_r) and dissipation factor ($\tan\delta$) of composites with different frequencies were measured and shown in Figures 4.26-4.31. It was found that the dielectric constant decreases and the dissipation factor increases at higher frequency. This is due to the

(a)

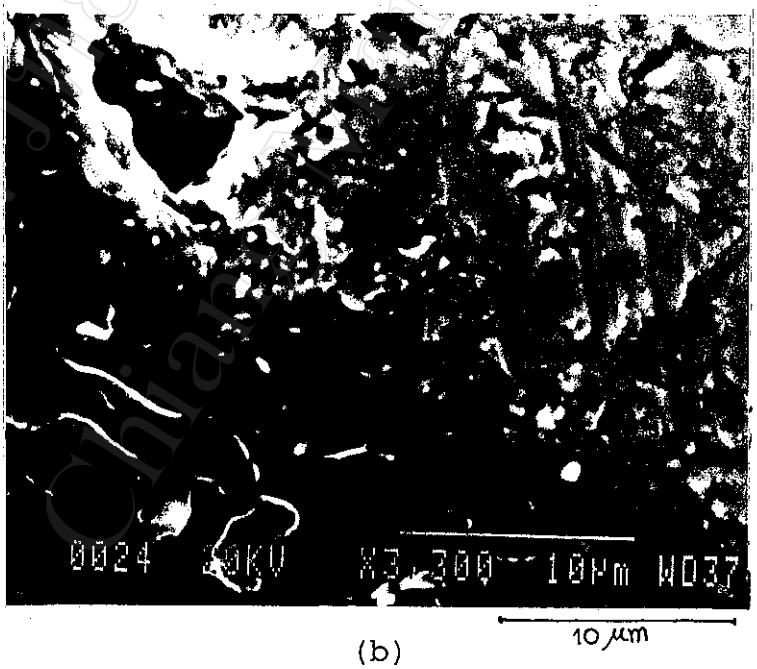

(b)

Figure 4.22 Scanning electron micrographs of the composites prepared by conventional method: (a) 50 vol%, (b) 60 vol%.

(a)

(b)

Figure 4.23 Scanning electron micrographs of centrifuging the PZT (from mixed oxides) and resin composites: (a) 60 vol%, (b) 65 vol%.

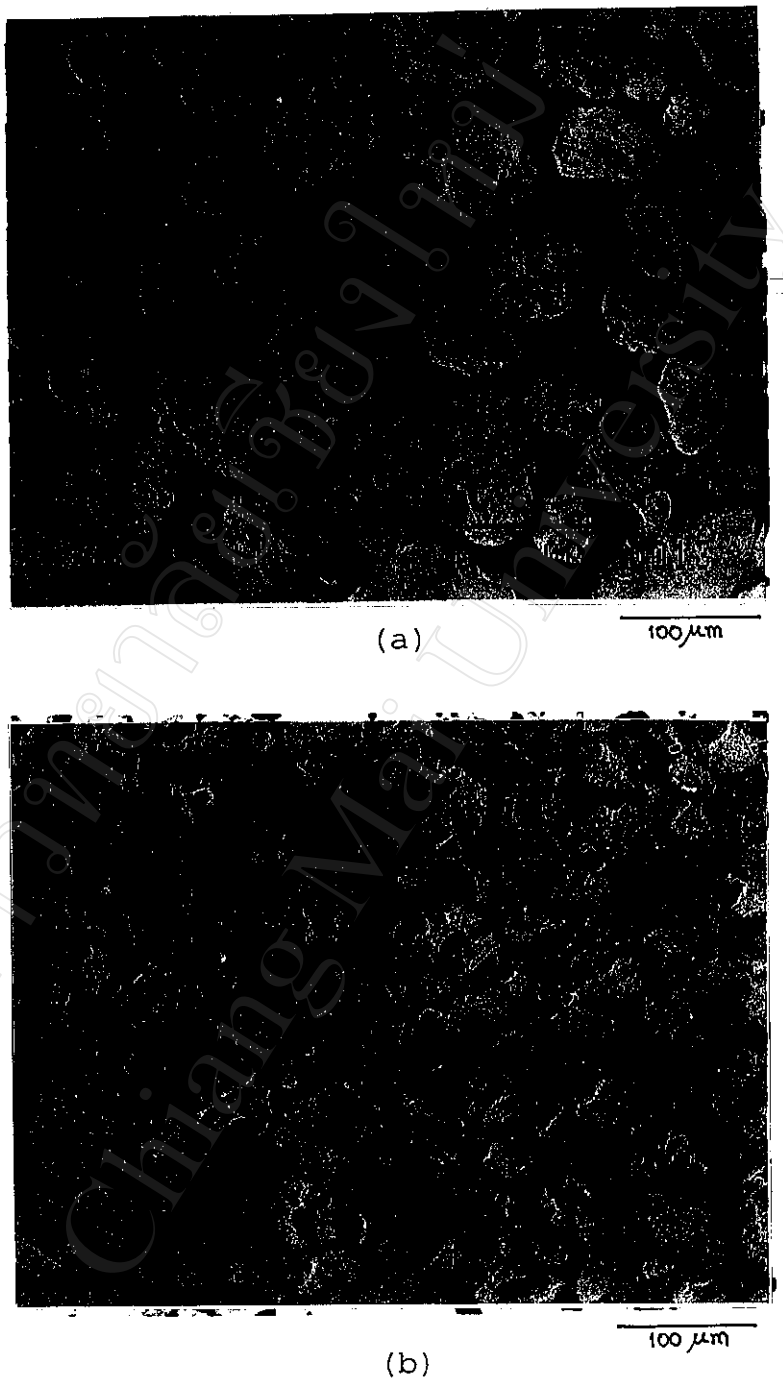

Figure 4.24 Scanning electron micrographs of centrifuging 40/30 PZT and resin composites: (a) 60 vol%, (b) 65 vol%.

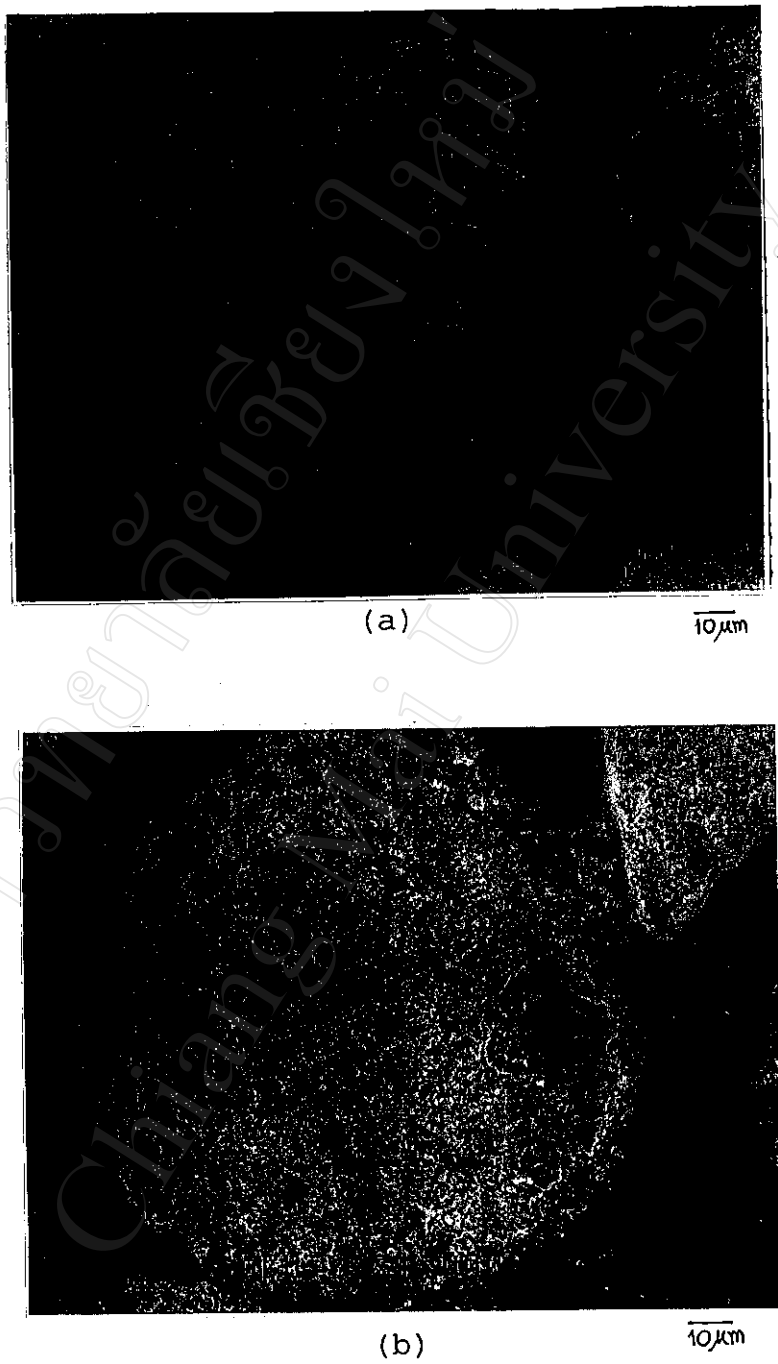

Figure 4.25 Scanning electron micrographs of PZT particles in the composites: (a) mixed oxides PZT, (b) 40/30 PZT.

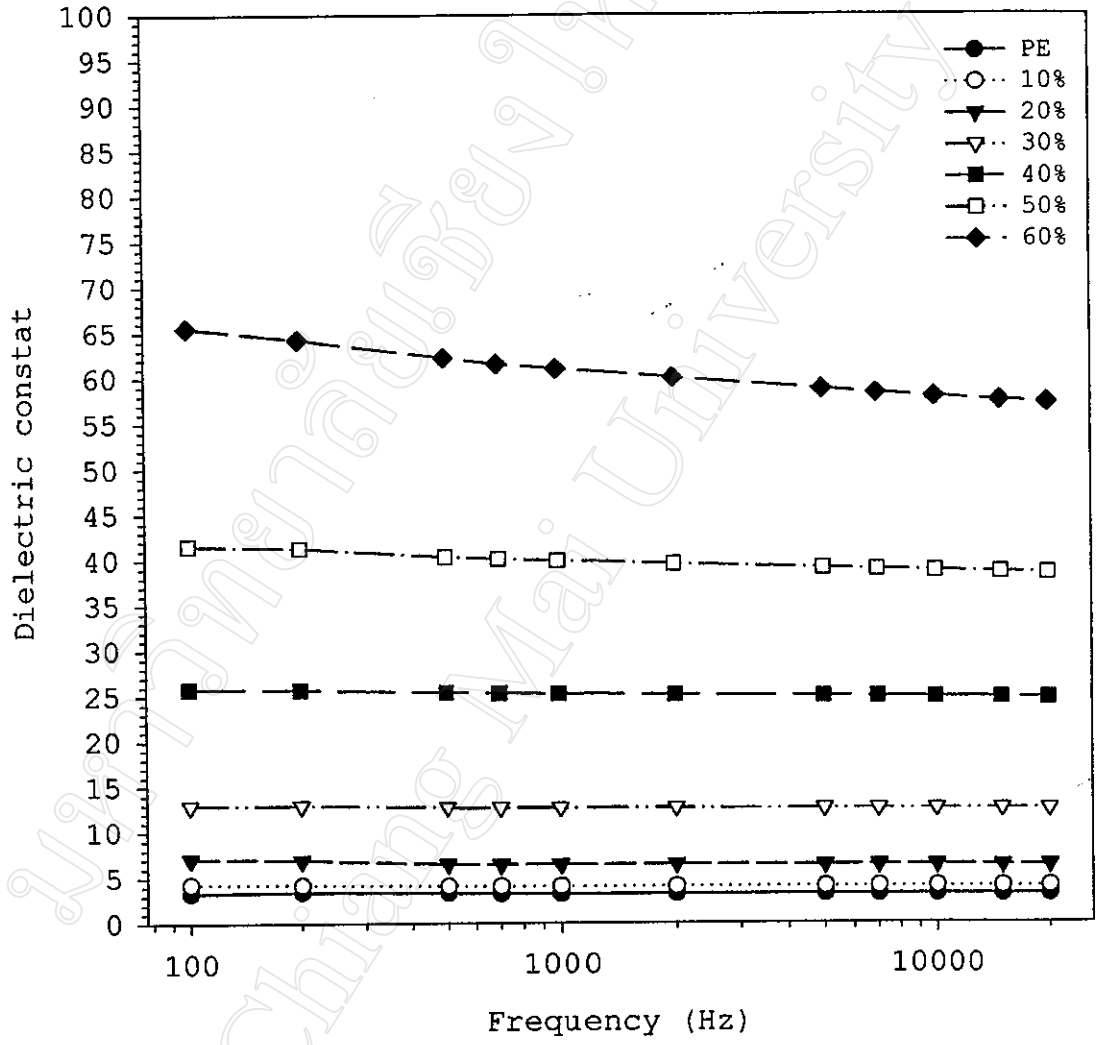

Figure 4.26 The plot of dielectric constant as a function of the frequency of composites prepared by conventional method.

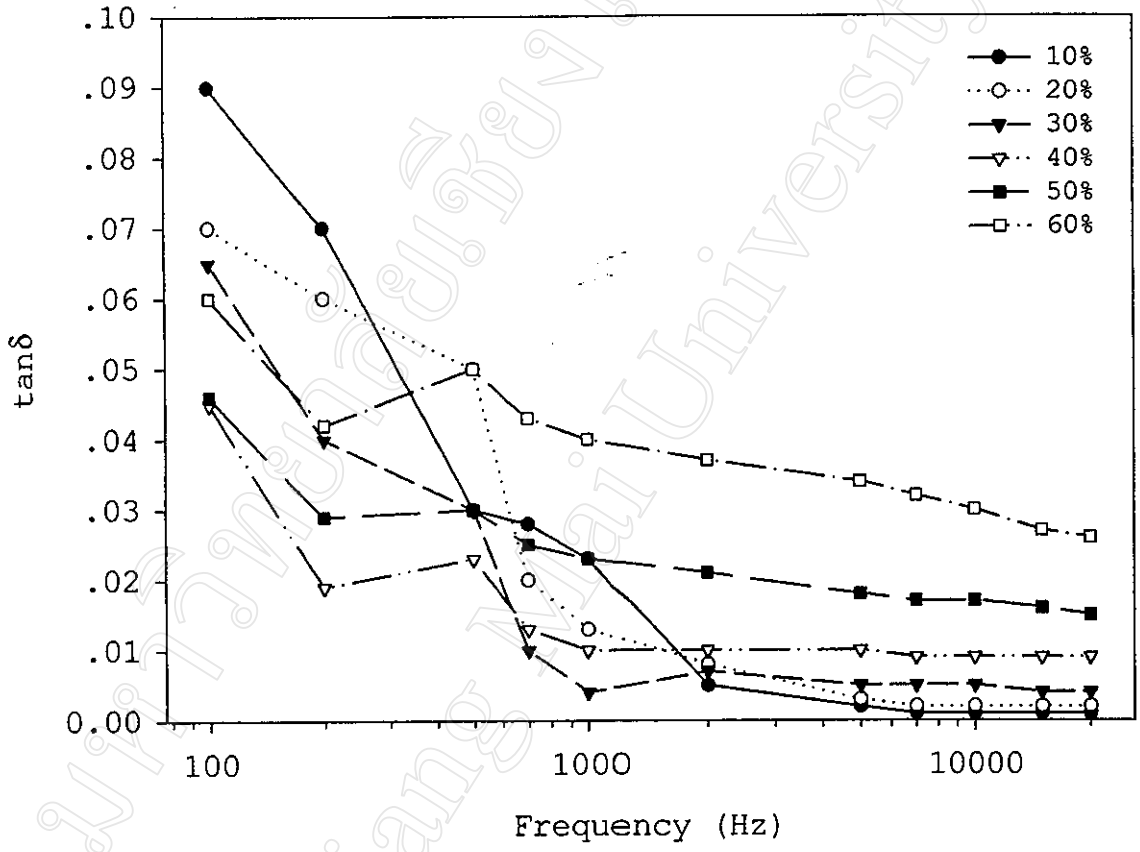

Figure 4.27 The plot of tanδ as a function of the frequency of composites prepared by conventional method.

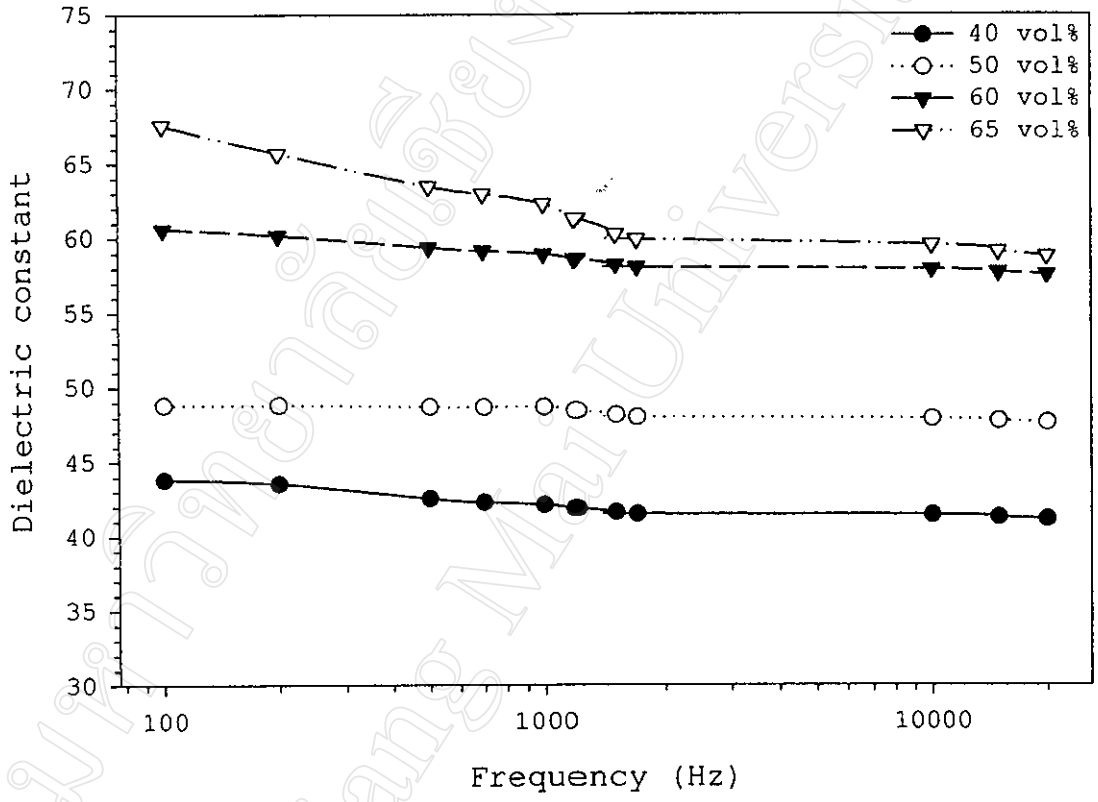

Figure 4.28 The plot of dielectric constant as a function of the frequency of mixed oxide PZT and resin composites prepared by centrifuge method.

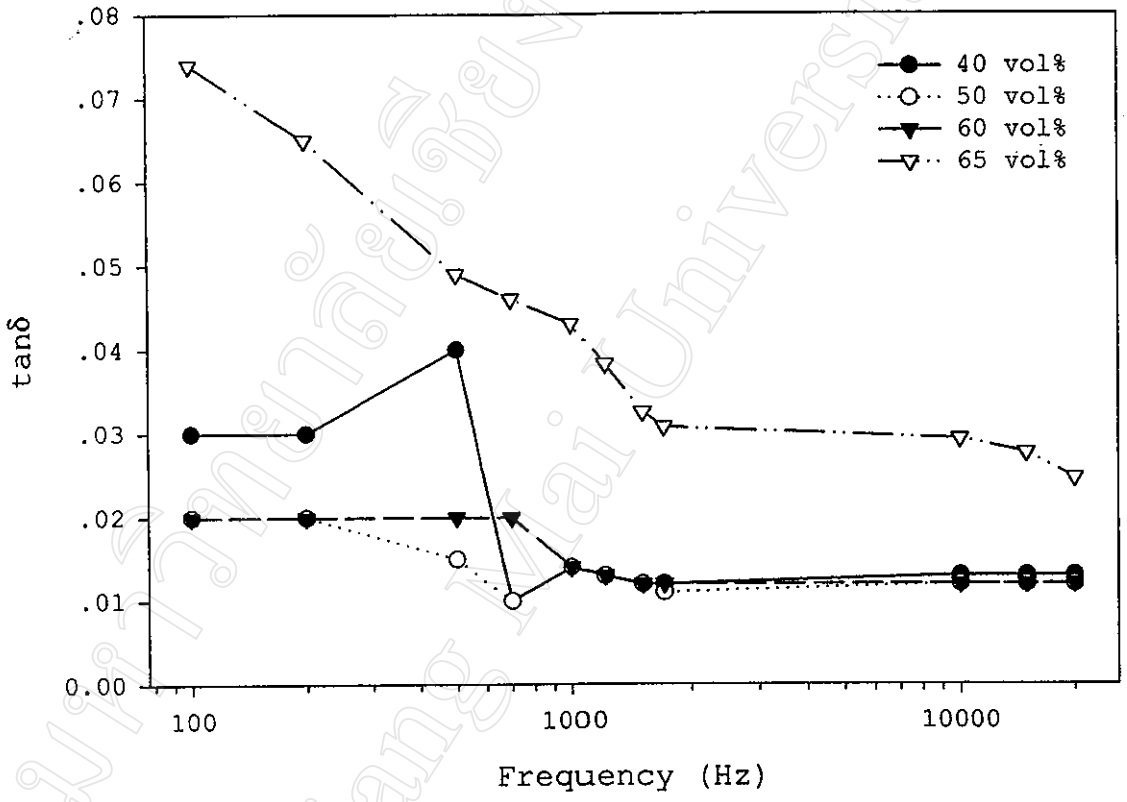

Figure 4.29 The plot of tanδ as a function of the frequency of mixed oxide PZT and resin composites prepared by centrifuge method.

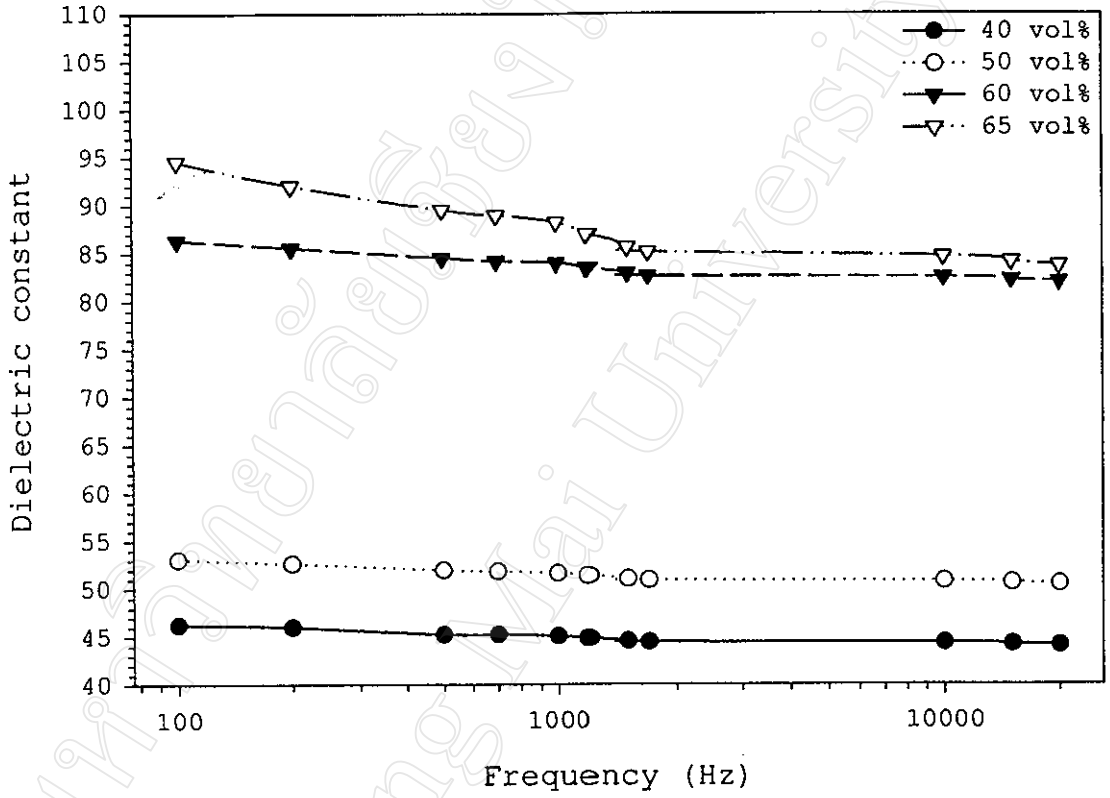

Figure 4.30 The plot of dielectric constant as a function of the frequency of 40/30 PZT and resin composites prepared by centrifuge method.

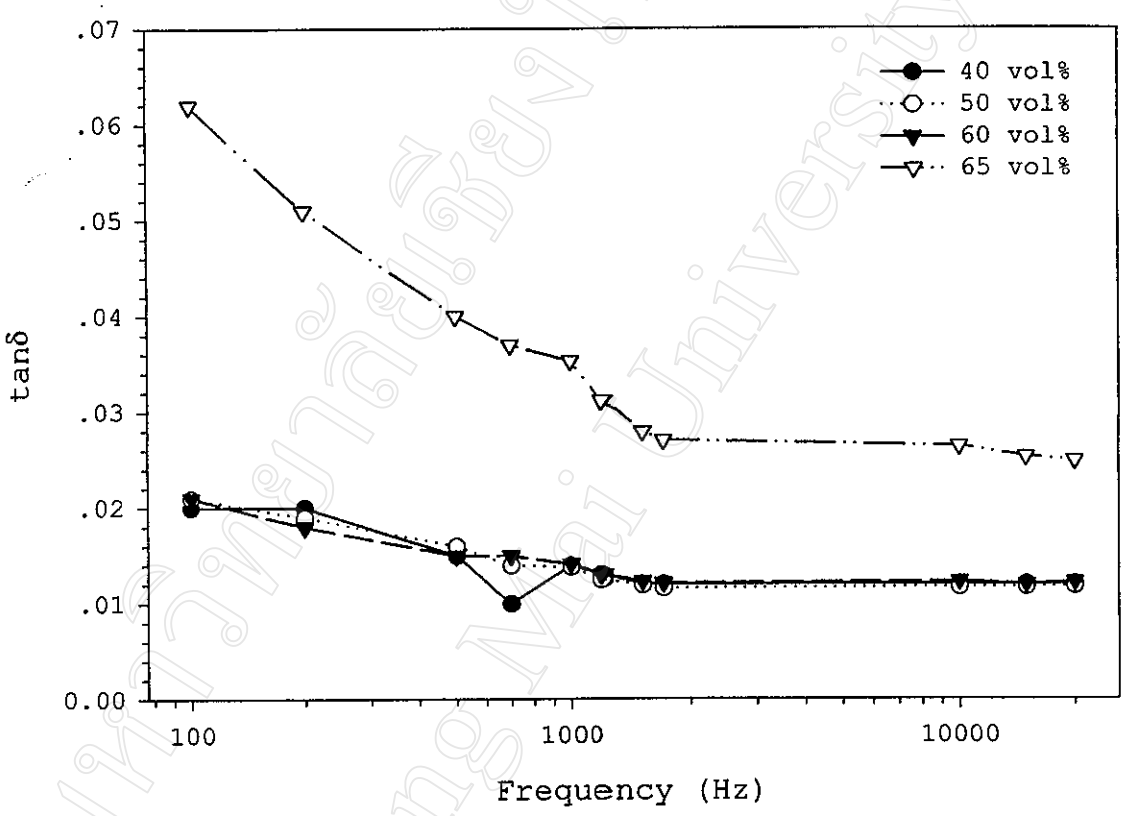

Figure 4.31 The plot of tanδ as a function of the frequency of 40/30 PZT and resin composites prepared by centrifuge method.

fact that the movement of the ions in atom is effected by their inertia in the high frequencies. The fluctuation of tan d under the frequency of 1 KHz of about 5-10% may be due to instrumental error. Table 4.4 shows the dielectric properties measured at frequency of 1 kHz and at room temperature. The result compared with that measured by Fries and Moulson[4] and Hanner et. al.[5]. The dielectric constant and dissipation factor are larger in the composites with higher percentage of the ceramic phase.

Table 4.4 Dielectric properties of the composites with different methods.

Sample	Vol%	ε_r	tanδ
Conventional PE+PZT	10	4.04	0.023
	20	6.43	0.013
	30	12.70	0.004
	40	25.23	0.010
	50	39.89	0.023
	60	61.01	0.040
Centrifuge Polyester resin+own PZT	40	42	0.014
	50	49	0.014
	60	59	0.014
	65	62	0.043
Centrifuge Polyester resin+40/30 PZT	40	45	0.0140
	50	52	0.0138
	60	84	0.0141
	65	88	0.0353
Thin film[4] PZT+PVC	60	134	0.23
PZT+Polyurethane[5]	60	51	0.02
	70	45	0.04

4.2.4 Piezoelectric Properties

All the composites were poled under a constant condition, in which the composites were held at 80 kV/cm for 15 min at the temperature of 70 °C, before measuring the piezoelectric properties. Table 4.5 shows the piezoelectric properties of 0-3 piezoceramic-polymer composites. It was found that the piezoelectric charge coefficient (d_{33}) and piezoelectric voltage coefficient (g_{33}) increase with the increasing of volume percentage of ceramic phase in both composites which were fabricated by conventional and centrifuge methods as described in Appendix C.2. The d_{33} value was highest (30 pC/N) in 65 volume% composite which was fabricated by the centrifuge method. However, d_{33} of the composite prepared by the centrifuge method was about 2 times higher than that of the composite prepared by the conventional method. This is due to the difference of polymer matrix materials and the method of fabrication. According to the dielectric constant model as discussed in Chapter 2, the electric field, E_1, action on ceramic phase is given by equation (2.8)

$$E_1 = 3K_2E_0/(K_1+3K_2) \qquad (4.1)$$

Where K_1 and K_2 are the dielectric constants of the ceramic filler and polymer matrix, respectively, and E_0 is the externally applied electric field. From the consideration of the dielectric constants of PE (K_2 = 4.48), polyester resin (K_2 = 3.212) and PZT (K_1 = 982), it can be clearly seen that the polarization in PZT particles in PZT-PE composites (prepared by conventional method) is less than in PZT-polyester resin composite (centrifuge method). Furthermore, the scanning electron micrographs of composites in Section 4.2.2 show the distribution of PZT particles which were more homogeneously mixed in the centrifuge method. Therefore, this result indicates that the centrifuge method has the tendency to possess higher piezoelectric properties of composites. All the d_{33} values obtained from the centrifuge method are comparable to those of Fries and Moulson[4], Hanner et. al.[5] and Cai et. al.[6], who used different preparation methods, such as calendering, painting and hot roller, respectively. However, these values of d_{33} in this work (10-29 pC/N) were less than that reported by Safari[7]. This is probably due to the poling method since Safari employed the corona method which can pole in higher field without breaking down the samples.

Table 4.5 Piezoelectric properties of the composites.

Samples	Vol%	d_{33} (pC/N)	g_{33} (mV-m/N)
Conventional PZT+PE	40	8	69.50
	50	11	49.70
	60	18	47.28
Centrifuge Own PZT+resin	40	11	29.58
	50	19	43.79
	60	25	47.85
	65	29	46.77
Centrifuge 40/30PZT+resin	40	10	25.10
	50	18	39.10
	60	26	34.96
	65	27	34.65
Thin film PZT+PVC[4]	60	29	24.44
PZT+Polyurethane Paint[5]	60	25	55.36
	70	28	70.27
Surface-treated PZT+PVDF[6]	65	33	82.82

4.2.5 Electromechanical Properties

The coupling factor (k_p) and the mechanical quality factor (Q_m) were calculated using formulae suggested by IRE standard piezoelectric measurement[8]. They were tabulated in table 4.6 together with that of others[9,10,11]. The values of k_p and Q_m obtained in the composites which were prepared by the centrifuge method were in the range of 0.33-0.45 and 4.4-9.9, respectively, which were comparable to those reported by Han et. al.[9]., Wersing[10] and Slayton and Setty[11]. Though their composites were prepared from colloidal PZT and epoxy, ceramic and plastic and single-particle-layer piezoelectric PZT and epoxy, respectively. However, these values cannot be obtained from conventional composite because the low value of d_{33} makes very difficult to measure the values of f_m and f_n.

Table 4.6 Showing k_p and Q_m value of the composites.

Sample	Vol%	k_p	Q_m
This work	40	0.29	4.43
	50	0.53	5.74
	60	0.35	9.20
	65	0.44	9.97
Han et. al.[9]	70	0.17	5-8
Wersing[10]	70	0.50	15
Slayton and Setty[11]	70	0.61	9.1

4.2.6 Acoustic Impedance

Table 4.7 shows the longitudinal velocity (c_L) obtained from the echo-shift method together with the Bulk modulus (K) values calculated using Equation (3.27). Both the longitudinal velocity and the Bulk modulus were found to increase with the increasing of the volumetric fraction of the PZT particles.

The acoustic impedance (Z) of the composite at various fraction of PZT are shown in Figure 4.32, together with those of Grewe et. al.[12], Wersing[10] and Slayton and Setty[11]. Furthermore the acoustic impedance was found to vary as the ceramic fraction in the composites. The Z-values are in the range of 6.80-11.41 Mrayls and 7.43-12.43 Mrayls for composites prepared by calendering and centrifuge methods, respectively. It is found that the results are comparable to that reported by Grewe et. al.[12], Wersing[10] and Slayton and Setty[11], though the fabrication routes are different. The Z data were analysed and fitted with Voigh, Reuss and Logarithmic models according to the methods suggested by Grewe et. al.[12]. The results show that the behaviour of Z of the composites fabricated by both methods is likely fitted with the Logarithmic model. The Z values fabricated in the centrifuge show higher than those of the samples prepared by the conventional method. This may be due to the density of the polyester resin is higher than that of polyethylene. These Z values indicate that these 0-3 piezoceramic-polymer composites have approximately 2-3 times lower acoustic impedance from pure PZT ceramic. Therefore, it is probably appropriate to use

as the transducer in water or human body which have low acoustic impedance as described in section 2.

Table 4.7 Physical properties (c_L and K) of the composites.

Samples	Vol%	c_L (m/s)	K ($kg/S^2.m$)
PE+PZT (40/30)	40	1852.8	12.60
	50	2032.8	18.66
	60	2270.2	25.90
	100	3585.5	101.44
Resin+PZT (40/30)	40	1995.7	14.83
	50	2219.6	21.49
	60	2277.1	26.16
	65	2349.7	29.21
	100	3585.5	101.44

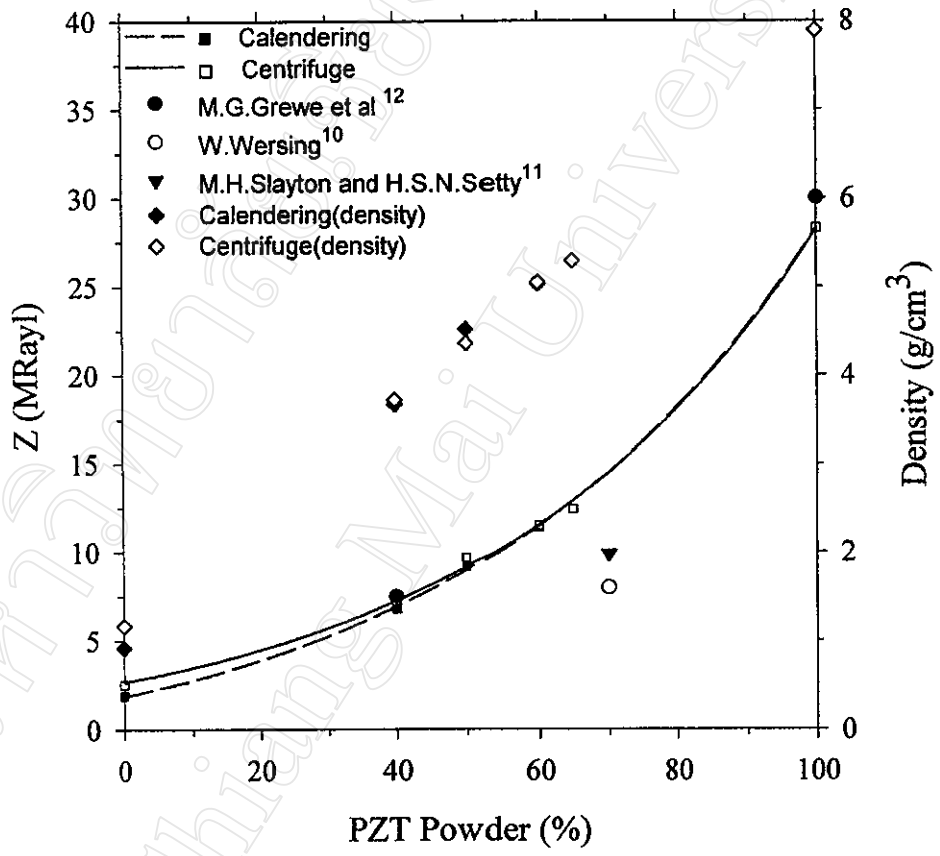

Figure 4.32 The acoustic impedance (Z) plotted against volume percentage of PZT powder.

REFERENCES

1. Powder Diffraction File, Card No. 33-784, Joint Committee on Powder Diffracton Standards, Swarthmire, PA
2. C. Whiston, "X-ray Methods", John Wiley & Sons, 87 (1987).
3. B.D. Cullity, "Elements of X-ray Diffraction", Addison-Wesley, Reading, MA, 102 (1987).
4. R. Fries and A.J. Moulson, *J. Matter. Sci. Mater. Electron.*, **5**, 238-243 (1994).
5. K.A. Hanner, A. Safari, R.E. Newnham and J. Runt, *Ferroelectrics*, **100**, 255 (1989).
6. X. Cai, C. Zhong, S. Zhang and H, Wang, *J. Mater. Sci. Lett.*, **16**, 253-254 (1997).
7. A. Safari, *J. Phys. III France*, **4**, 1129-1149 (1994).
8. "IRE Standards on Piezoelectric Crystals: Measurements of Piezoelectric Ceramics". *Proc. IRE*, **49**, 1161-1169 (1961).
9. K.H. Han, A. Safari and R.E. Riman, *J. Am. Ceram. Soc.*, **74**, 1669-1702 (1991).

10. W. Wersing, *IEEE Inter. Symp. Appl. Ferroelectrics*, 212-213 (1986).

11. M.H. Slayton and H.S.N. Setty, *IEEE Inter. Symp. Appl. Ferroelectrics*, 90-92 (1990).

12. M.G. Grewe, T.R. Gururaja, R.E. Newnham and T.R. Shrout, *IEEE Ultrasonic Symp.*, 713-716 (1989).